Sparse reconstruction-based contribution for multiple fault isolation by KPCA

Gilles Mourot, Maya Kallas, Kwami Anani, Didier Maquin

Research Center for Automatic Control of Nancy (CRAN)
2, avenue de la Forêt de Haye
54500 Vandœuvre, France

MED'18: The 26th Mediterranean Conference on Control and Automation

Zadar, Croatia, June 19-22, 2018

Context of the study

- It addresses the problem of multiple fault isolation based on kernel principal component analysis

Context of the study

- It addresses the problem of multiple fault isolation based on kernel principal component analysis
- It proposes a sparse fault estimation method to evaluate the so-called reconstruction-based contribution

Context of the study

- It addresses the problem of multiple fault isolation based on kernel principal component analysis
- It proposes a sparse fault estimation method to evaluate the so-called reconstruction-based contribution
- The fault magnitude estimation is formulated as an optimization problem under nonnegativity and sum-to-one constraints. A multiplicative iterative scheme is proposed to solve it.

Context of the study

- It addresses the problem of multiple fault isolation based on kernel principal component analysis
- It proposes a sparse fault estimation method to evaluate the so-called reconstruction-based contribution
- The fault magnitude estimation is formulated as an optimization problem under nonnegativity and sum-to-one constraints. A multiplicative iterative scheme is proposed to solve it.
- The effectiveness of the proposed method is demonstrated on the simulated continuous stirred tank reactor (CSTR) process.

Basics of Kernel PCA

Basics of Kernel PCA

- Data matrix : n measurement vectors x_i collected under normal operation :

$$X = [x_1, \cdots, x_n]^\top \in \mathbb{R}^{n \times m}$$

Basics of Kernel PCA

- Data matrix : n measurement vectors x_i collected under normal operation :

$$X = [x_1, \cdots, x_n]^\top \in \mathbb{R}^{n \times m}$$

- Nonlinear mapping function from the input space $\mathscr{X}$ into the feature space $\mathscr{H}$:

$$\varphi : \mathscr{X} \mapsto \mathscr{H}$$
$$x_i \mapsto \varphi_i = \varphi(x_i) \in \mathbb{R}^h$$

Basics of Kernel PCA

- Data matrix : n measurement vectors x_i collected under normal operation :

$$X = [x_1, \cdots, x_n]^\top \in \mathbb{R}^{n \times m}$$

- Nonlinear mapping function from the input space $\mathscr{X}$ into the feature space $\mathscr{H}$:

$$\varphi : \mathscr{X} \mapsto \mathscr{H}$$
$$x_i \mapsto \varphi_i = \varphi(x_i) \in \mathbb{R}^h$$

- Matrix gathering the mapped vectors are written as follows :

$$\Phi = [\varphi_1, \cdots, \varphi_n]^\top \in \mathbb{R}^{n \times h}$$

Basics of Kernel PCA

- Data matrix : n measurement vectors x_i collected under normal operation :

$$X = [x_1, \cdots, x_n]^\top \in \mathbb{R}^{n \times m}$$

- Nonlinear mapping function from the input space $\mathscr{X}$ into the feature space $\mathscr{H}$:

$$\varphi : \mathscr{X} \mapsto \mathscr{H}$$
$$x_i \mapsto \varphi_i = \varphi(x_i) \in \mathbb{R}^h$$

- Matrix gathering the mapped vectors are written as follows :

$$\Phi = [\varphi_1, \cdots, \varphi_n]^\top \in \mathbb{R}^{n \times h}$$

- Empirical covariance matrix :

$$S = \frac{1}{n-1} \Phi^\top \Phi$$

Basics of Kernel PCA

- The primal formulation of KPCA $\rightarrow$ eigenvalue/eigenvector problem :

$$\frac{1}{n-1}\,\Phi^{\top}\Phi\,v_i = \lambda_i\,v_i \qquad i = 1,\ldots,n$$

v_i and λ_i are the eigenvectors and eigenvalues of the covariance matrix S

Basics of Kernel PCA

- The primal formulation of KPCA $\rightarrow$ eigenvalue/eigenvector problem :

$$\frac{1}{n-1}\,\Phi^{\top}\Phi\,v_i = \lambda_i\,v_i \qquad i = 1,\ldots,n$$

  v_i and λ_i are the eigenvectors and eigenvalues of the covariance matrix S

- However, $\varphi(\cdot)$ does not need to be explicitly defined

Basics of Kernel PCA

- The primal formulation of KPCA $\rightarrow$ eigenvalue/eigenvector problem :

$$\frac{1}{n-1}\,\Phi^\top \Phi\, v_i = \lambda_i\, v_i \qquad i = 1, \ldots, n$$

  v_i and λ_i are the eigenvectors and eigenvalues of the covariance matrix S

- However, $\varphi(\cdot)$ does not need to be explicitly defined

- The Gram matrix $K = \Phi\ \Phi^\top$ is then evaluated from a kernel

$$\kappa(x_i, x_j) = \varphi(x_i)^\top \varphi(x_j)$$

Basics of Kernel PCA

- The primal formulation of KPCA $\rightarrow$ eigenvalue/eigenvector problem :

$$\frac{1}{n-1}\,\Phi^\top \Phi\, v_i = \lambda_i\, v_i \qquad i = 1, \ldots, n$$

  v_i and λ_i are the eigenvectors and eigenvalues of the covariance matrix S

- However, $\varphi(\cdot)$ does not need to be explicitly defined

- The Gram matrix $K = \Phi\ \Phi^\top$ is then evaluated from a kernel

$$\kappa(x_i, x_j) = \varphi(x_i)^\top \varphi(x_j)$$

- In the following, the Gaussian kernel is used :

$$\kappa(x_i, x_j) = \exp\left(-\frac{(x_i - x_j)^T (x_i - x_j)}{2\,c}\right)$$

  where c is the kernel dispersion parameter.

Basics of Kernel PCA

- The primal formulation of KPCA $\rightarrow$ eigenvalue/eigenvector problem :

$$\frac{1}{n-1}\,\Phi^\top \Phi\, v_i = \lambda_i\, v_i \qquad i = 1, \ldots, n$$

  v_i and λ_i are the eigenvectors and eigenvalues of the covariance matrix S

- However, $\varphi(\cdot)$ does not need to be explicitly defined

- The Gram matrix $K = \Phi\ \Phi^\top$ is then evaluated from a kernel

$$\kappa(x_i, x_j) = \varphi(x_i)^\top \varphi(x_j)$$

- In the following, the Gaussian kernel is used :

$$\kappa(x_i, x_j) = \exp\left(-\frac{(x_i - x_j)^T (x_i - x_j)}{2\,c}\right)$$

  where c is the kernel dispersion parameter.

- The covariance matrix S and $\frac{1}{n-1}\,K$ have the same r non-zero eigenvalues

$$S = \frac{1}{n-1}\Phi^\top \Phi$$

Basics of Kernel PCA

- Their eigenvectors are related by :

$$V = \Phi^\top A \qquad A = \frac{1}{\sqrt{n-1}} U \Lambda^{-1/2}$$

U and V are the matrices of the eigenvectors associated to the diagonal matrix of eigenvalues Λ

Basics of Kernel PCA

- Their eigenvectors are related by :

$$V = \Phi^\top A \qquad A = \frac{1}{\sqrt{n-1}} U \Lambda^{-1/2}$$

U and V are the matrices of the eigenvectors associated to the diagonal matrix of eigenvalues Λ

- By choosing a number ℓ of principal components, the feature space is decomposed into the principal and residual subspaces, spanned respectively by $\hat{V}$ (the ℓ first eigenvectors of V corresponding to the ℓ largest eigenvalues) and $\tilde{V}$ (the $r-\ell$ last eigenvectors of V). The same partitioning is considered for U and Λ.

Basics of Kernel PCA

- Their eigenvectors are related by :

$$V = \Phi^\top A \qquad A = \frac{1}{\sqrt{n-1}} U \Lambda^{-1/2}$$

U and V are the matrices of the eigenvectors associated to the diagonal matrix of eigenvalues Λ

- By choosing a number ℓ of principal components, the feature space is decomposed into the principal and residual subspaces, spanned respectively by $\hat{V}$ (the ℓ first eigenvectors of V corresponding to the ℓ largest eigenvalues) and $\tilde{V}$ (the $r-\ell$ last eigenvectors of V). The same partitioning is considered for U and Λ.

Fault detection using SPE

Basics of Kernel PCA

- Their eigenvectors are related by :

$$V = \Phi^\top A \qquad A = \frac{1}{\sqrt{n-1}} U \Lambda^{-1/2}$$

U and V are the matrices of the eigenvectors associated to the diagonal matrix of eigenvalues Λ

- By choosing a number ℓ of principal components, the feature space is decomposed into the principal and residual subspaces, spanned respectively by $\hat{V}$ (the ℓ first eigenvectors of V corresponding to the ℓ largest eigenvalues) and $\tilde{V}$ (the $r-\ell$ last eigenvectors of V). The same partitioning is considered for U and Λ.

Fault detection using SPE

- The projection of x onto the residual subspace is evaluated as :

$$\tilde{t}(x) = \tilde{V}^\top \varphi(x)$$

- Their eigenvectors are related by :

$$V = \Phi^\top A \qquad A = \frac{1}{\sqrt{n-1}} U \Lambda^{-1/2}$$

U and V are the matrices of the eigenvectors associated to the diagonal matrix of eigenvalues Λ

- By choosing a number ℓ of principal components, the feature space is decomposed into the principal and residual subspaces, spanned respectively by $\hat{V}$ (the ℓ first eigenvectors of V corresponding to the ℓ largest eigenvalues) and $\tilde{V}$ (the $r-\ell$ last eigenvectors of V). The same partitioning is considered for U and Λ.

Fault detection using SPE

- The projection of x onto the residual subspace is evaluated as :

$$\tilde{t}(x) = \tilde{V}^\top \varphi(x)$$

- The corresponding detection index SPE is given by :

$$SPE(x) = \tilde{t}^\top(x)\tilde{t}(x) = 1 - \kappa^\top(x)\,\hat{Q}\,\kappa(x)$$

where

$$\hat{Q} = \hat{A}\hat{A}^\top \qquad \kappa(x) = [\kappa(x_1, x), \cdots, \kappa(x_n, x)]^\top$$

Sparse reconstruction-based contribution

Problem position

Sparse reconstruction-based contribution

Problem position

- Reconstructed observation (assuming known the set R of faulty variables)

$$z_R = x - \Xi_R \, f_R$$

where Ξ_R is the matrix of fault directions with 1 to indicate the faulty variables and 0 for the other variables.

Sparse reconstruction-based contribution

Problem position

- Reconstructed observation (assuming known the set R of faulty variables)

$$z_R = x - \Xi_R \, f_R$$

where Ξ_R is the matrix of fault directions with 1 to indicate the faulty variables and 0 for the other variables.

- Estimation of fault magnitudes

$$\hat{f}_R = \arg\min_{f_R} SPE(z_R)$$

Sparse reconstruction-based contribution

Problem position

- Reconstructed observation (assuming known the set R of faulty variables)

$$z_R = x - \Xi_R \, f_R$$

where Ξ_R is the matrix of fault directions with 1 to indicate the faulty variables and 0 for the other variables.

- Estimation of fault magnitudes

$$\hat{f}_R = \arg\min_{f_R} SPE(z_R)$$

- Reconstruction-based contribution of subset R

$$RBC_R = SPE(x) - SPE(\hat{z}_R)$$

where $\hat{z}_R$ is the reconstructed observation obtained by replacing $\hat{f}_R$ in z_R.

Sparse reconstruction-based contribution

Problem position

Sparse reconstruction-based contribution

Problem position

- Estimation of fault magnitudes

$$\hat{f}_R = \arg\min_{f_R} SPE(z_R)$$

Sparse reconstruction-based contribution

Problem position

- Estimation of fault magnitudes

$$\hat{f}_R = \arg\min_{f_R} SPE(z_R)$$

Resolution method

- This minimization problem needs the SPE to be derived with respect to f_R

$$\frac{\partial SPE(z_R)}{\partial f_R} = -\frac{2}{c}\sum_{j=1}^{n} \beta_j \Xi_R^\top (z_R - x_j)$$

with

$$\beta_j = \kappa(z_R, x_j)\, \xi_j^\top\, \hat{Q}\, \kappa(z_R)$$

and ξ_j is the j^{th} column of the identity matrix.

Sparse reconstruction-based contribution

Solution

$$\hat{f}_R = \sum_{j=1}^{n} \hat{\alpha}_j \Xi_R^\top \left(x - x_j\right)$$

with

$$\hat{\alpha}_j = \frac{\kappa(\hat{z}_R, x_j)\, \xi_j^\top \hat{Q}\, \kappa(\hat{z}_R)}{\sum_{t=1}^{n} \kappa(\hat{z}_R, x_t)\, \xi_j^\top \hat{Q}\, \kappa(\hat{z}_R)}, \qquad \hat{z}_R = x - \Xi_R \hat{f}_R$$

Sparse reconstruction-based contribution

Solution

$$\hat{f}_R = \sum_{j=1}^{n} \hat{\alpha}_j \Xi_R^\top \left(x - x_j\right)$$

with

$$\hat{\alpha}_j = \frac{\kappa(\hat{z}_R, x_j)\, \xi_j^\top \hat{Q}\, \kappa(\hat{z}_R)}{\sum_{t=1}^{n} \kappa(\hat{z}_R, x_t)\, \xi_j^\top \hat{Q}\, \kappa(\hat{z}_R)}, \qquad \hat{z}_R = x - \Xi_R \hat{f}_R$$

$\rightarrow$ it's an implicit form as $\hat{f}_R$ depends on $\hat{z}_R$ which itself depends on $\hat{f}_R$

Sparse reconstruction-based contribution

Solution

$$\hat{f}_R = \sum_{j=1}^{n} \hat{\alpha}_j \Xi_R^\top \left(x - x_j\right)$$

with

$$\hat{\alpha}_j = \frac{\kappa(\hat{z}_R, x_j)\, \xi_j^\top \hat{Q}\, \kappa(\hat{z}_R)}{\sum_{t=1}^{n} \kappa(\hat{z}_R, x_t)\, \xi_j^\top \hat{Q}\, \kappa(\hat{z}_R)}, \qquad \hat{z}_R = x - \Xi_R \hat{f}_R$$

$\rightarrow$ it's an implicit form as $\hat{f}_R$ depends on $\hat{z}_R$ which itself depends on $\hat{f}_R$

A solution can be obtained using a iterative fixed-point scheme

Sparse reconstruction-based contribution

Solution

$$\hat{f}_R = \sum_{j=1}^{n} \hat{\alpha}_j \Xi_R^\top \left(x - x_j\right)$$

with

$$\hat{\alpha}_j = \frac{\kappa(\hat{z}_R, x_j)\, \xi_j^\top \hat{Q}\, \kappa(\hat{z}_R)}{\sum_{t=1}^{n} \kappa(\hat{z}_R, x_t)\, \xi_j^\top \hat{Q}\, \kappa(\hat{z}_R)}, \qquad \hat{z}_R = x - \Xi_R \hat{f}_R$$

$\rightarrow$ it's an implicit form as $\hat{f}_R$ depends on $\hat{z}_R$ which itself depends on $\hat{f}_R$

A solution can be obtained using a iterative fixed-point scheme

Remarks

Sparse reconstruction-based contribution

Solution

$$\hat{f}_R = \sum_{j=1}^{n} \hat{\alpha}_j \Xi_R^\top \left(x - x_j\right)$$

with

$$\hat{\alpha}_j = \frac{\kappa(\hat{z}_R, x_j)\, \xi_j^\top \hat{Q}\, \kappa(\hat{z}_R)}{\sum_{t=1}^{n} \kappa(\hat{z}_R, x_t)\, \xi_j^\top \hat{Q}\, \kappa(\hat{z}_R)}, \qquad \hat{z}_R = x - \Xi_R \hat{f}_R$$

$\rightarrow$ it's an implicit form as $\hat{f}_R$ depends on $\hat{z}_R$ which itself depends on $\hat{f}_R$

A solution can be obtained using a iterative fixed-point scheme

Remarks

The estimate $\hat{f}_R$ is a linear combination of the differences between training data and faulty measurement along the reconstruction directions $\Xi_R^\top$.

Sparse reconstruction-based contribution

Solution

$$\hat{f}_R = \sum_{j=1}^{n} \hat{\alpha}_j \Xi_R^\top (x - x_j)$$

with

$$\hat{\alpha}_j = \frac{\kappa(\hat{z}_R, x_j)\, \xi_j^\top \hat{Q}\, \kappa(\hat{z}_R)}{\sum_{t=1}^{n} \kappa(\hat{z}_R, x_t)\, \xi_j^\top \hat{Q}\, \kappa(\hat{z}_R)}, \qquad \hat{z}_R = x - \Xi_R \hat{f}_R$$

$\rightarrow$ it's an implicit form as $\hat{f}_R$ depends on $\hat{z}_R$ which itself depends on $\hat{f}_R$

A solution can be obtained using a iterative fixed-point scheme

Remarks

The estimate $\hat{f}_R$ is a linear combination of the differences between training data and faulty measurement along the reconstruction directions $\Xi_R^\top$.

The coefficients $\hat{\alpha}_j$, acting as training data contributions to the estimation, could be positive or negative but their sum is one, which may lead to compensation in the linear combination.

Sparse reconstruction-based contribution

Estimation subject to nonnegativity and sum-to-one constraints (reformulation [1])

$$\hat{f}_R = \arg\min_{\alpha} SPE(z_R)$$

with

$$\begin{cases} z_R & = & x - \Xi_R f_R \\ f_R & = & \sum_{j=1}^{n} \alpha_j \Xi_R^{\top}(x - x_j) \end{cases}$$

subject to the constraints :

$$\begin{cases} \alpha_j & \geq 0, \qquad j = 1, \ldots, n \\ \sum_{j=1}^{n} \alpha_j & = 1 \end{cases}$$

1. M. Kallas, P. Honeine, C. Richard, C. Francis, and H. Amoud, "Non-negativity constraints on the pre-image for pattern recognition with kernel machines," Pattern Recognition, vol. 46, no. 11, pp. 3066–3080, 2013.

Estimation subject to nonnegativity and sum-to-one constraints (reformulation)

To solve more easily this fully constrained nonlinear optimization problem, a procedure similar to that proposed by Lanteri [2] in 2011 is used :

- We introduce the following variable change :

$$\alpha_j = \frac{\omega_j}{\sum_{i=1}^{n} \omega_i} \quad \text{with} \quad \omega_j \geq 0, j = 1, \ldots, n$$

- We proceed to the minimization with respect to the new variable ω_j, subject to nonnegativity constraint only, using a component-wise gradient descent,

- We come back to the initial variables α_j.

2. H. Lantéri, C. Theys, and C. Richard,"Nonnegative matrix factorization with regularization and sparsity-enforcing terms," in 4th IEEE International Workshop on Computational Advances in Multi-Sensor Adaptive Processing (CAMSAP), December 2011.

Estimation subject to nonnegativity and sum-to-one constraints

The Lagrangian function for nonnegativity constraint problem is then given by :

$$\mathscr{L}(\omega,\mu) = SPE(z_R) - \mu^\top \omega$$

At the optimum (ω^*,μ^*), the Karush-Kuhn-Tucker (KKT) conditions reduce to :

$$\omega_j^* \left.\frac{\partial SPE(z_R)}{\partial \omega_j}\right|_{\omega_j=\omega_j^*} = 0 \qquad j = 1,\ldots,n$$

$$\left.\frac{\partial SPE(z_R)}{\partial \omega_j}\right|_{\omega_j=\omega_j^*} \geq 0 \qquad j = 1,\ldots,n$$

$$\omega_j^* \geq 0 \qquad j = 1,\ldots,n$$

Sparse reconstruction-based contribution

Estimation subject to nonnegativity and sum-to-one constraints

To solve these nonlinear equations, the following gradient descent updating scheme is defined :

$$\omega_j^{(t+1)} = \omega_j^{(t)} - \eta_j^{(t)} g_j\left(\omega_j^{(t)}\right) \omega_j^{(t)} \frac{\partial SPE(z_R^{(t)})}{\partial \omega_j}$$

where

$\eta_j^{(t)}$ is the step-size which controls the convergence of the algorithm,

$g_j\left(\omega_j^{(t)}\right) > 0$ is a positive function scaling the gradient

Estimation subject to nonnegativity and sum-to-one constraints

To solve these nonlinear equations, the following gradient descent updating scheme is defined :

$$\omega_j^{(t+1)} = \omega_j^{(t)} - \eta_j^{(t)} g_j\left(\omega_j^{(t)}\right) \omega_j^{(t)} \frac{\partial SPE(z_R^{(t)})}{\partial \omega_j}$$

where

$\eta_j^{(t)}$ is the step-size which controls the convergence of the algorithm,

$g_j\left(\omega_j^{(t)}\right) > 0$ is a positive function scaling the gradient

This above equation could be re-written as follows :

$$\omega_j^{(t+1)} = \omega_j^{(t)} m_j^{(t)}$$

with

$$m_j^{(t)} = 1 - \eta_j^{(t)} g_j(\omega_j^{(t)}) \frac{\partial SPE(z_R^{(t)})}{\partial \omega_j}$$

Estimation subject to nonnegativity and sum-to-one constraints

To solve these nonlinear equations, the following gradient descent updating scheme is defined :

$$\omega_j^{(t+1)} = \omega_j^{(t)} - \eta_j^{(t)} g_j\left(\omega_j^{(t)}\right) \omega_j^{(t)} \frac{\partial SPE(z_R^{(t)})}{\partial \omega_j}$$

where

$\eta_j^{(t)}$ is the step-size which controls the convergence of the algorithm,

$g_j\left(\omega_j^{(t)}\right) > 0$ is a positive function scaling the gradient

This above equation could be re-written as follows :

$$\omega_j^{(t+1)} = \omega_j^{(t)} m_j^{(t)}$$

with

$$m_j^{(t)} = 1 - \eta_j^{(t)} g_j(\omega_j^{(t)}) \frac{\partial SPE(z_R^{(t)})}{\partial \omega_j}$$

To avoid an expensive step-size computation for each component of ω, in practice, a single step-size $\eta^{(t)}$ is chosen.

Simulation on the CSTR benchmark [3]

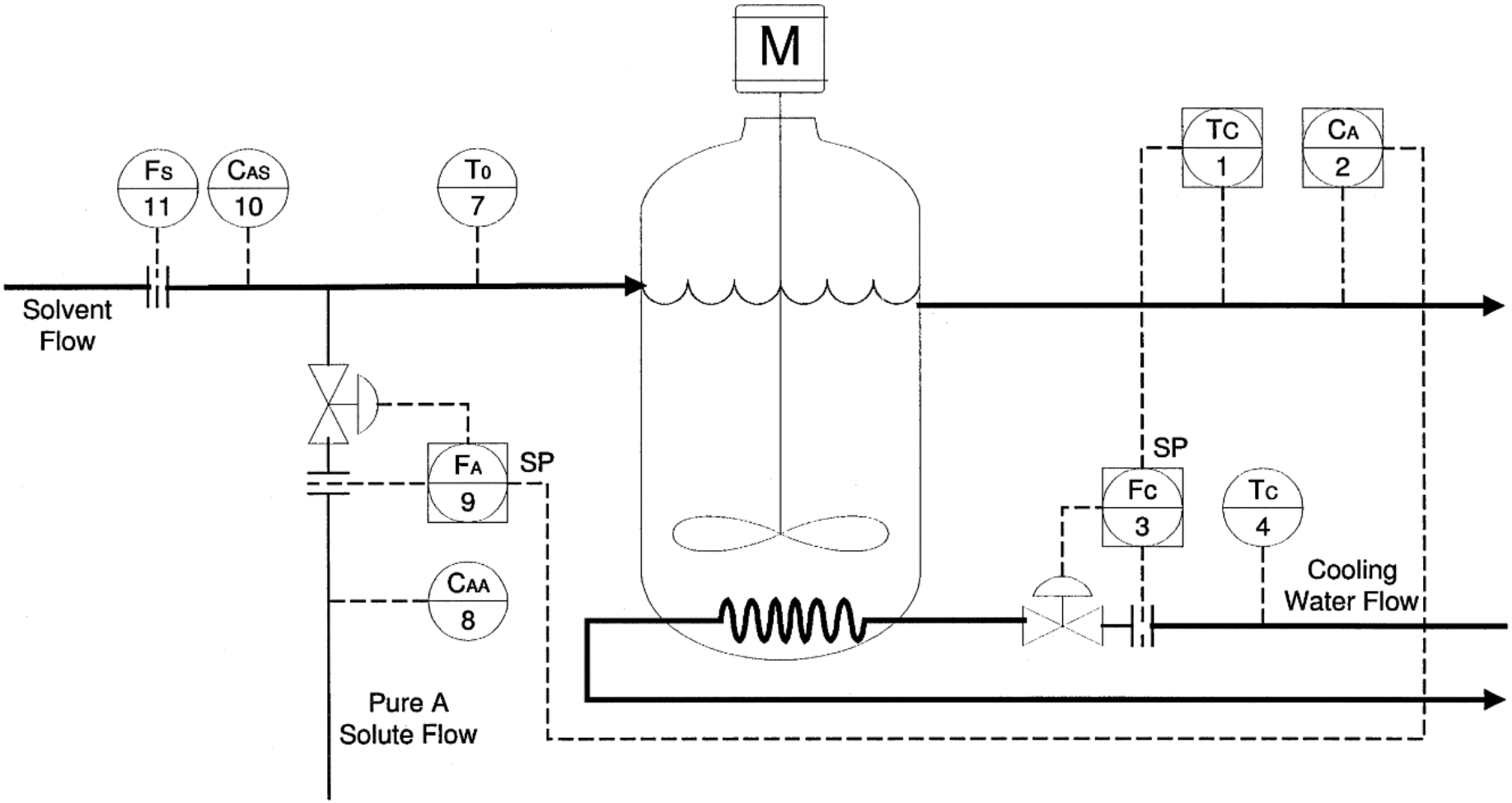

FIGURE – CSTR scheme

3. S. Yoon and J. F. MacGregor, "Fault diagnosis with multivariate statistical models part i : using steady state fault signatures," Journal of Process Control, vol. 11, no. 4, pp. 387–400, 2001.

Simulation on the CSTR benchmark

Assumptions

- The reactor contains well mixed constituents and has constant physical properties
- A first order reaction is taken into consideration where reactant A is mixed with a solvent in order to obtain a product B

Simulation on the CSTR benchmark

Assumptions

- The reactor contains well mixed constituents and has constant physical properties
- A first order reaction is taken into consideration where reactant A is mixed with a solvent in order to obtain a product B

Model of the CSTR (mass and energy balance)

$$\frac{dC_A}{dt} = \frac{F}{V}C_{A0} - \frac{F}{V}C_A - k_0 \mathrm{e}^{-\frac{E}{RT}} C_A$$

$$V\rho C_P \frac{dT}{dt} = \rho C_P F(T_0 - T) + (-\Delta H_r) V k_0 \mathrm{e}^{-\frac{E}{RT}} C_A - \frac{aF_C^{b+1}}{F_C + \frac{aF_C^b}{(2\rho_C C_{PC})}}(T - T_C)$$

V is the volume of the tank, F the input flow rate, ΔH_r the heat of reaction, k_0 the reaction velocity constant, ρ the reaction mixture density, ρ_C the coolant density, C_P the volumetric heat capacity, C_{PC} the coolant capacity, E the activation energy, R the gas constant, the temperature T, the cooling water temperature T_C, the inlet temperature T_0, the coolant flow F_C, and the outlet concentration C_A, a and b are constant coefficients.

Simulation on the CSTR benchmark

- Overall inlet concentration :

$$C_{A0} = \frac{C_{AA} F_A + C_{AS} F_S}{F_A + F_S}$$

with the inlet concentrations C_{AA} and C_{AS}, the solvent flow F_S, and the reactant flow F_A.

Simulation on the CSTR benchmark

- Overall inlet concentration :

$$C_{A0} = \frac{C_{AA} F_A + C_{AS} F_S}{F_A + F_S}$$

  with the inlet concentrations C_{AA} and C_{AS}, the solvent flow F_S, and the reactant flow F_A.

- T is controlled by F_C using a proportional-integral (PI) controller.

Simulation on the CSTR benchmark

- Overall inlet concentration :

$$C_{A0} = \frac{C_{AA} F_A + C_{AS} F_S}{F_A + F_S}$$

  with the inlet concentrations C_{AA} and C_{AS}, the solvent flow F_S, and the reactant flow F_A.

- T is controlled by F_C using a proportional-integral (PI) controller.

- Nine variables are measured for fault detection and isolation process defining an observation x at each instant with :

$$x = [T_C \;\; T_0 \;\; C_{AA} \;\; C_{AS} \;\; F_S \;\; F_C \;\; C_A \;\; T \;\; F_A]^\top$$

Simulation on the CSTR benchmark

- Overall inlet concentration :

$$C_{A0} = \frac{C_{AA} F_A + C_{AS} F_S}{F_A + F_S}$$

with the inlet concentrations C_{AA} and C_{AS}, the solvent flow F_S, and the reactant flow F_A.

- T is controlled by F_C using a proportional-integral (PI) controller.
- Nine variables are measured for fault detection and isolation process defining an observation x at each instant with :

$$x = [T_C \;\; T_0 \;\; C_{AA} \;\; C_{AS} \;\; F_S \;\; F_C \;\; C_A \;\; T \;\; F_A]^\top$$

- A set of 100 observations were used during training, where KPCA is applied using a Gaussian kernel with $c = 0.36$.

Simulation on the CSTR benchmark

- Overall inlet concentration :

$$C_{A0} = \frac{C_{AA} F_A + C_{AS} F_S}{F_A + F_S}$$

  with the inlet concentrations C_{AA} and C_{AS}, the solvent flow F_S, and the reactant flow F_A.

- T is controlled by F_C using a proportional-integral (PI) controller.

- Nine variables are measured for fault detection and isolation process defining an observation x at each instant with :

$$x = [T_C \;\; T_0 \;\; C_{AA} \;\; C_{AS} \;\; F_S \;\; F_C \;\; C_A \;\; T \;\; F_A]^\top$$

- A set of 100 observations were used during training, where KPCA is applied using a Gaussian kernel with $c = 0.36$.

- 28 principal components were needed to define the KPCA model and a detection threshold was estimated with a value of 0.21.

Simulation on the CSTR benchmark

Fault affecting the inlet temperature T_0

A step of $1.5K$ on the inlet temperature T_0 starting at instant 51 was added.

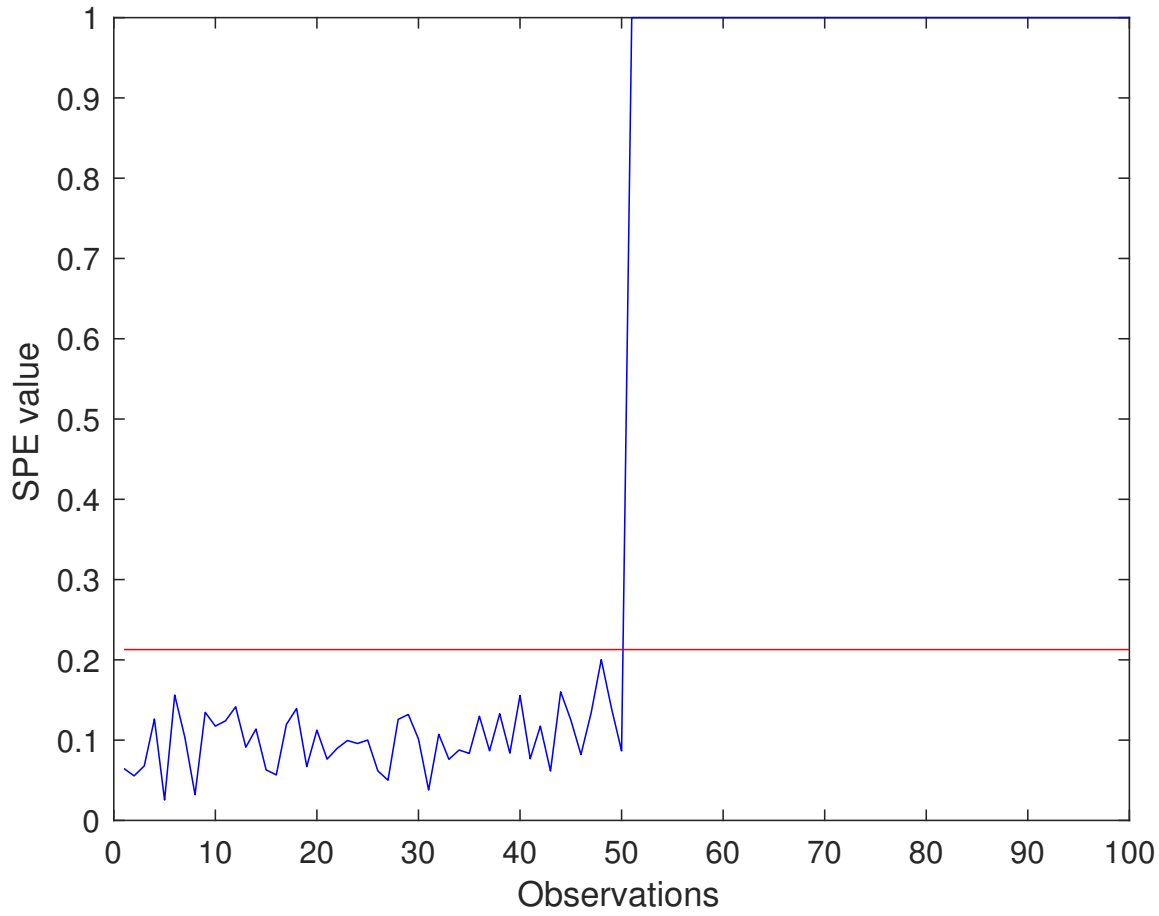

FIGURE – Detection of fault on the inlet temperature T_0

Fault affecting the inlet temperature T_0

Cumulative RBC (sum of RBC over the 50 faulty observations).
SPE after reconstruction of T_0 : 0.08 (< 0.21).

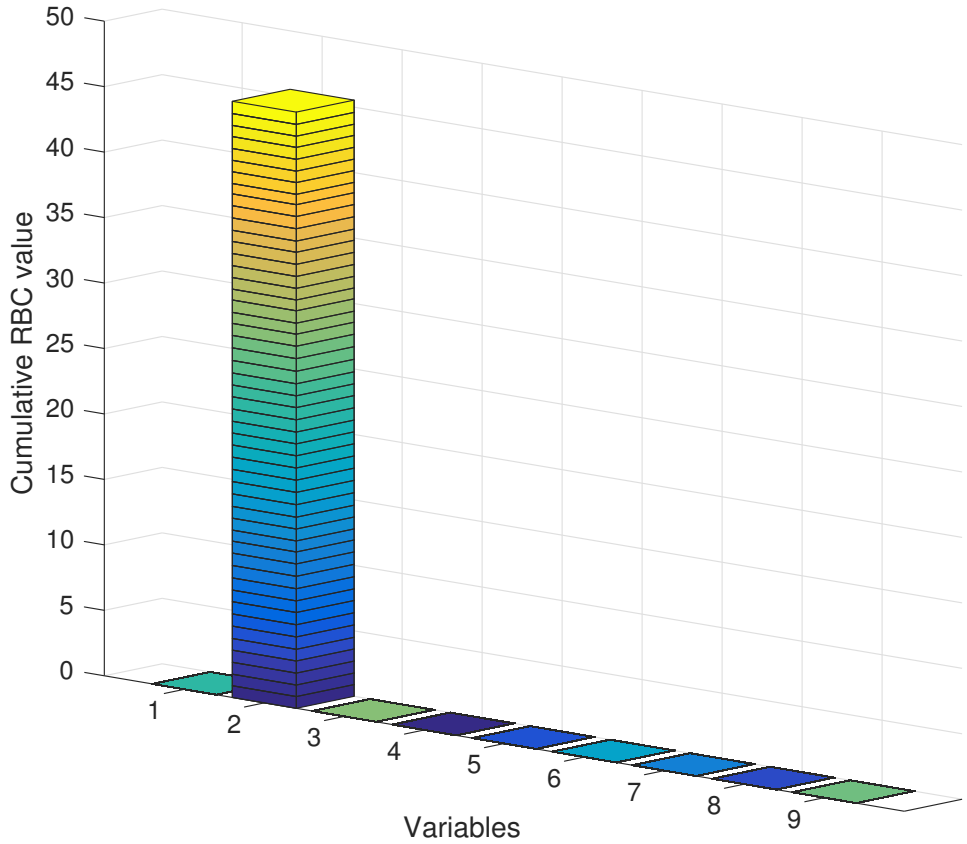

FIGURE – Cumulative RBC for fault affecting T_0

Simulation on the CSTR benchmark

Fault affecting the temperature T

A step of $1K$ on the temperature measurement T starting at instant 51 was added.

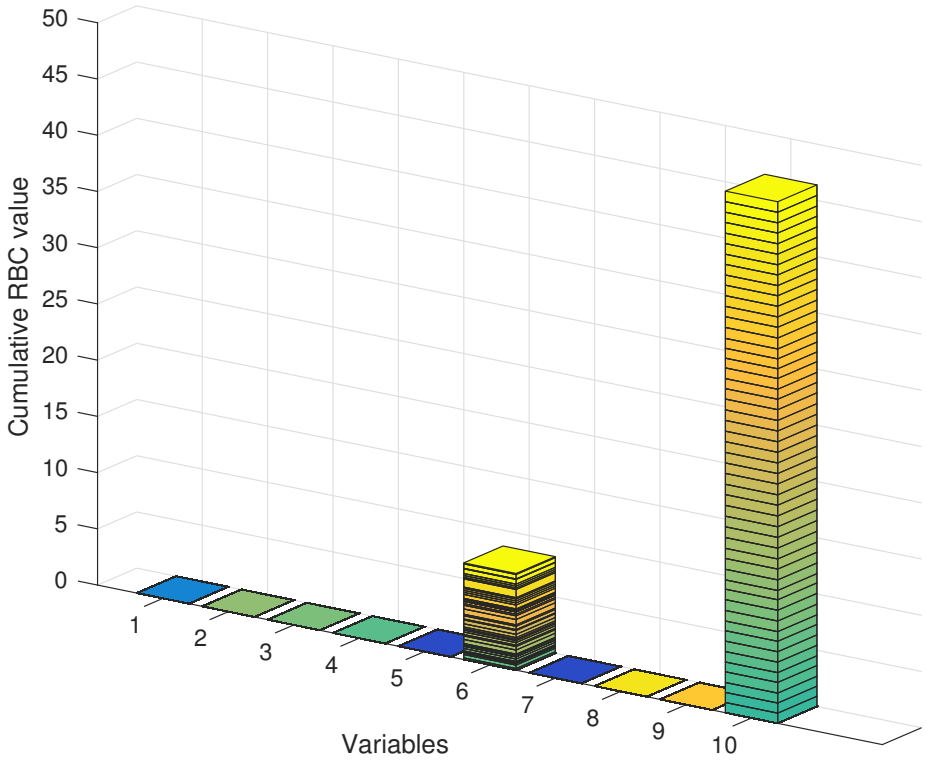

FIGURE – Cumulative RBC for fault affecting T

Simulation on the CSTR benchmark

Fault affecting the temperature T

A step of $1K$ on the temperature measurement T starting at instant 51 was added.

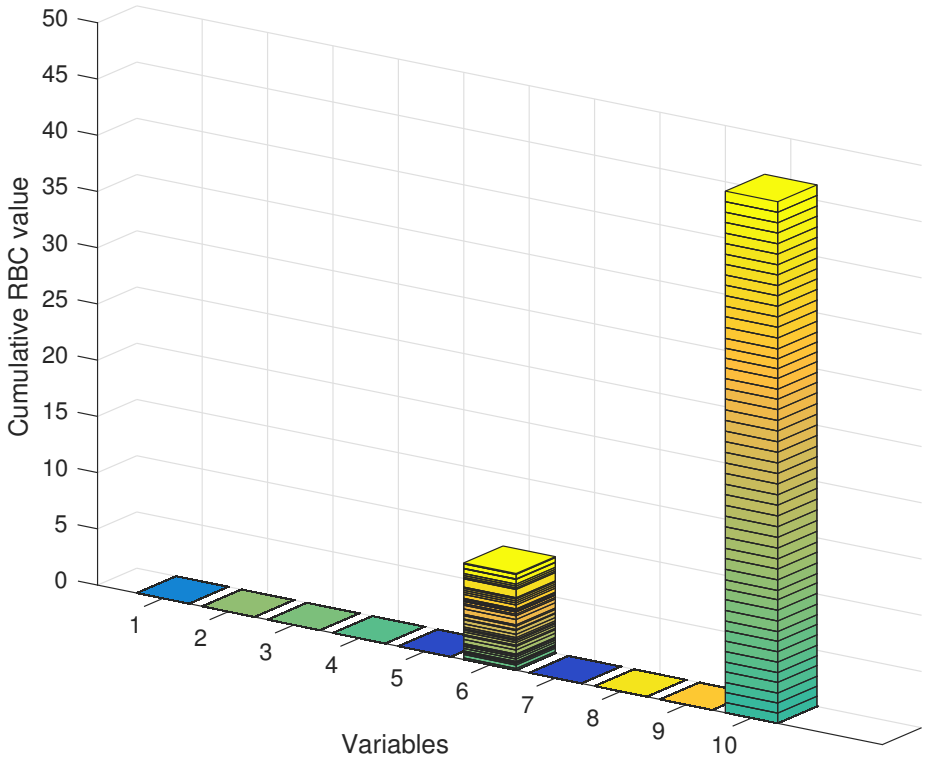

FIGURE – Cumulative RBC for fault affecting T

Among the nine reconstructed variables, variable 6, F_C has the higher contribution.

Simulation on the CSTR benchmark

Fault affecting the temperature T

A step of $1K$ on the temperature measurement T starting at instant 51 was added.

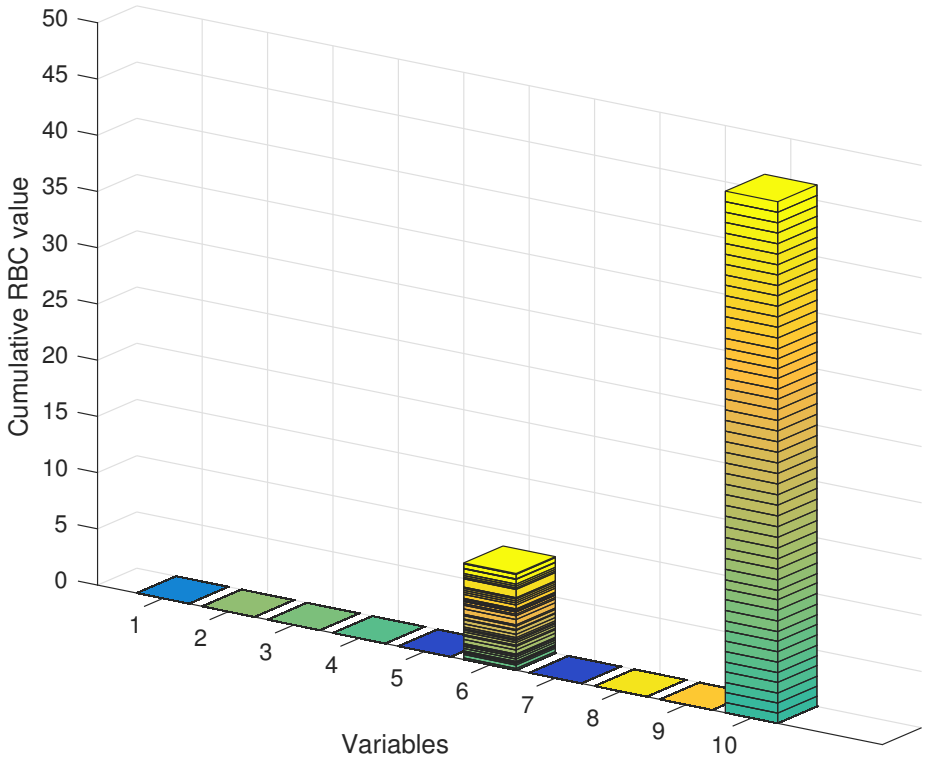

FIGURE – Cumulative RBC for fault affecting T

Among the nine reconstructed variables, variable 6, F_C has the higher contribution.

The SPE evaluated after the reconstruction of F_C is equal to 0.82 that is greater to the threshold 0.21.

Simulation on the CSTR benchmark

Fault affecting the temperature T

A step of $1K$ on the temperature measurement T starting at instant 51 was added.

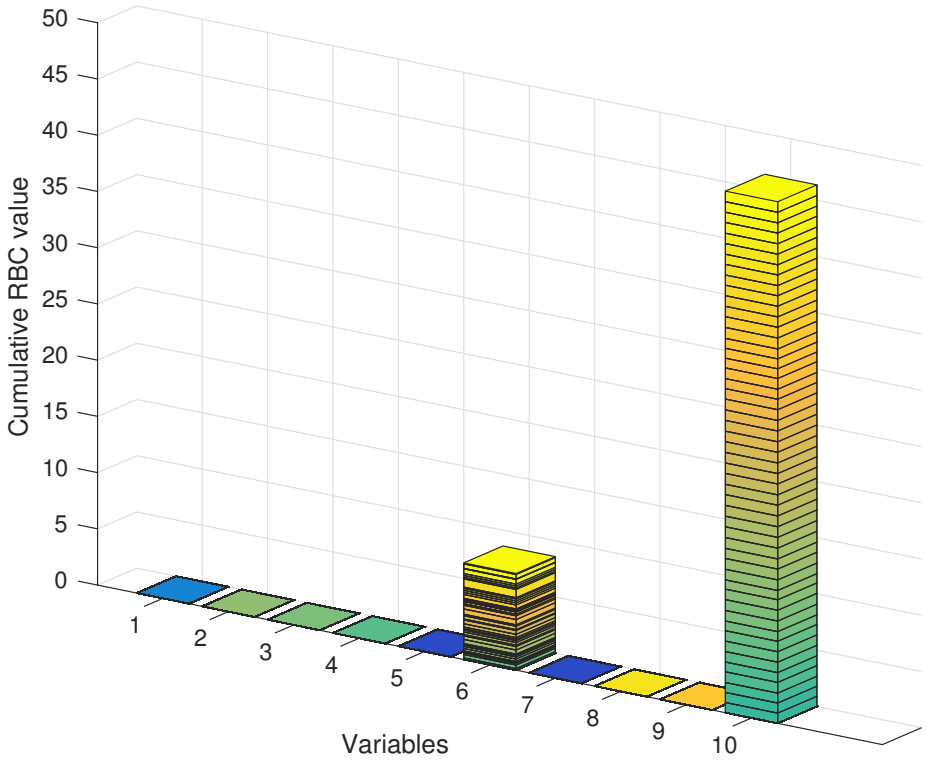

FIGURE – Cumulative RBC for fault affecting T

Among the nine reconstructed variables, variable 6, F_C has the higher contribution.

The SPE evaluated after the reconstruction of F_C is equal to 0.82 that is greater to the threshold 0.21.

We cannot conclude that the fault occurs on F_C.

Simulation on the CSTR benchmark

Fault affecting the temperature T

A step of $1K$ on the temperature measurement T starting at instant 51 was added.

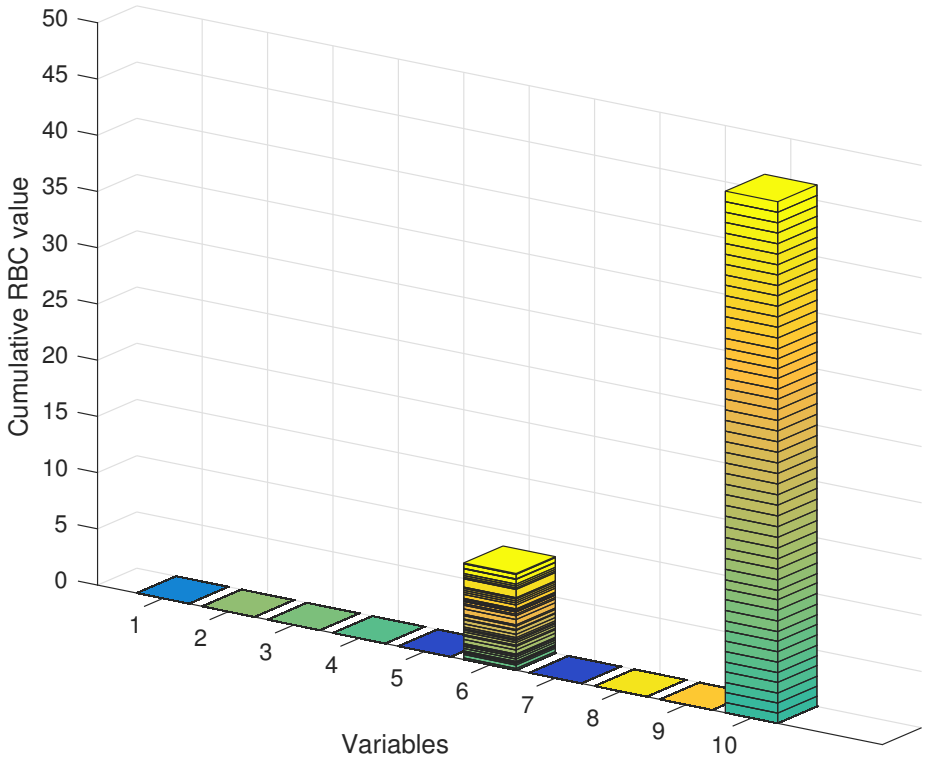

FIGURE – Cumulative RBC for fault affecting T

Among the nine reconstructed variables, variable 6, F_C has the higher contribution.

The SPE evaluated after the reconstruction of F_C is equal to 0.82 that is greater to the threshold 0.21.

We cannot conclude that the fault occurs on F_C.

$\rightarrow$ it's necessary to seek a combination of different variables for which the SPE after reconstruction is less than the threshold

Simulation on the CSTR benchmark

Fault affecting the temperature T

A step of $1K$ on the temperature measurement T starting at instant 51 was added.

Simulation on the CSTR benchmark

Fault affecting the temperature T

A step of $1K$ on the temperature measurement T starting at instant 51 was added.

- The fault on T has a complex effect, indeed T is controlled by a PI regulator.

Simulation on the CSTR benchmark

Fault affecting the temperature T

A step of $1K$ on the temperature measurement T starting at instant 51 was added.

- The fault on T has a complex effect, indeed T is controlled by a PI regulator.
- The increase of the temperature measurement involves an increase of the coolant flow F_C.

Simulation on the CSTR benchmark

Fault affecting the temperature T

A step of $1K$ on the temperature measurement T starting at instant 51 was added.

- The fault on T has a complex effect, indeed T is controlled by a PI regulator.
- The increase of the temperature measurement involves an increase of the coolant flow F_C.
- However, the real temperature inside the reactor is less than the one needed for a normal operation.

Simulation on the CSTR benchmark

Fault affecting the temperature T

A step of $1K$ on the temperature measurement T starting at instant 51 was added.

- The fault on T has a complex effect, indeed T is controlled by a PI regulator.
- The increase of the temperature measurement involves an increase of the coolant flow F_C.
- However, the real temperature inside the reactor is less than the one needed for a normal operation.
- In consequence, the concentration C_A of the product at the output increases too.

Simulation on the CSTR benchmark

Fault affecting the temperature T

A step of $1K$ on the temperature measurement T starting at instant 51 was added.

- The fault on T has a complex effect, indeed T is controlled by a PI regulator.
- The increase of the temperature measurement involves an increase of the coolant flow F_C.
- However, the real temperature inside the reactor is less than the one needed for a normal operation.
- In consequence, the concentration C_A of the product at the output increases too.

In conclusion, the three variables T, F_C and C_A are affected by the considered sensor fault.

Simulation on the CSTR benchmark

Fault affecting the temperature T

A step of $1K$ on the temperature measurement T starting at instant 51 was added.

- The fault on T has a complex effect, indeed T is controlled by a PI regulator.
- The increase of the temperature measurement involves an increase of the coolant flow F_C.
- However, the real temperature inside the reactor is less than the one needed for a normal operation.
- In consequence, the concentration C_A of the product at the output increases too.

In conclusion, the three variables T, F_C and C_A are affected by the considered sensor fault.

By reconstructing simultaneously these three variables, the corresponding SPE (after reconstruction) falls down to 0.07 (which is clearly under the given threshold).

Simulation on the CSTR benchmark

Fault affecting the temperature T

A step of $1K$ on the temperature measurement T starting at instant 51 was added.

- The fault on T has a complex effect, indeed T is controlled by a PI regulator.
- The increase of the temperature measurement involves an increase of the coolant flow F_C.
- However, the real temperature inside the reactor is less than the one needed for a normal operation.
- In consequence, the concentration C_A of the product at the output increases too.

In conclusion, the three variables T, F_C and C_A are affected by the considered sensor fault.

By reconstructing simultaneously these three variables, the corresponding SPE (after reconstruction) falls down to 0.07 (which is clearly under the given threshold).

This result shows the importance of reconstructing more than one variables.

Simulation on the CSTR benchmark

- This result can be advantageously compared with that of Alcala and Quin [3]

3. C.F. Alcala and S.J. Qin, "Reconstruction-based contribution for process monitoring with kernel principal component analysis," Industrial & Engineering Chemistry Research, vol. 49, no. 17, pp. 7849-7857, 2010.

Simulation on the CSTR benchmark

- This result can be advantageously compared with that of Alcala and Quin [3]
- The used indicators are not exactly the same ; they used an average RBC using the square of the estimated fault magnitude

3. C.F. Alcala and S.J. Qin, "Reconstruction-based contribution for process monitoring with kernel principal component analysis," Industrial & Engineering Chemistry Research, vol. 49, no. 17, pp. 7849-7857, 2010.

Simulation on the CSTR benchmark

- This result can be advantageously compared with that of Alcala and Quin [3]
- The used indicators are not exactly the same ; they used an average RBC using the square of the estimated fault magnitude
- Based on their analysis, it could have been enough to reconstruct the coolant flow F_C (which is not the correct decision, i.e. isolation of fault)

3. C.F. Alcala and S.J. Qin, "Reconstruction-based contribution for process monitoring with kernel principal component analysis," Industrial & Engineering Chemistry Research, vol. 49, no. 17, pp. 7849-7857, 2010.

Simulation on the CSTR benchmark

- This result can be advantageously compared with that of Alcala and Quin [3]
- The used indicators are not exactly the same ; they used an average RBC using the square of the estimated fault magnitude
- Based on their analysis, it could have been enough to reconstruct the coolant flow F_C (which is not the correct decision, i.e. isolation of fault)
- In case of fault with complex effect, the fault isolation will be subject to a structural-functional analysis of the system in order to determine the candidate subsets of variables to be reconstructed.

3. C.F. Alcala and S.J. Qin, "Reconstruction-based contribution for process monitoring with kernel principal component analysis," Industrial & Engineering Chemistry Research, vol. 49, no. 17, pp. 7849-7857, 2010.

Conclusion and perspectives

- A sparse fault estimation method to evaluate the reconstruction-based contribution for multiple fault isolation has been developed

Conclusion and perspectives

- A sparse fault estimation method to evaluate the reconstruction-based contribution for multiple fault isolation has been developed
- The fault magnitude estimation, formulated as an optimization problem under nonnegativity and sum-to-one constraints, is solved using a multiplicative iterative scheme

Conclusion and perspectives

- A sparse fault estimation method to evaluate the reconstruction-based contribution for multiple fault isolation has been developed
- The fault magnitude estimation, formulated as an optimization problem under nonnegativity and sum-to-one constraints, is solved using a multiplicative iterative scheme
- A toy example (issued from the literature dedicated to that subject) based on a CSTR model illustrates the effectiveness of the proposed method

Conclusion and perspectives

- A sparse fault estimation method to evaluate the reconstruction-based contribution for multiple fault isolation has been developed
- The fault magnitude estimation, formulated as an optimization problem under nonnegativity and sum-to-one constraints, is solved using a multiplicative iterative scheme
- A toy example (issued from the literature dedicated to that subject) based on a CSTR model illustrates the effectiveness of the proposed method
- A future work will aim at determining the useful potential reconstruction directions in order to handle the combinatorial nature of multiple fault isolation

Who am I ?

Didier Maquin

Professor of Automatic Control
Université de Lorraine

Ecole Nationale Supérieure d'Electricité et de Mécanique

Ecole Nationale Supérieure des Mines de Nancy

Centre de Recherche en Automatique de Nancy

Contact : didier.maquin@univ-lorraine.fr

More details ?

Personal web site : `http://www.cran.univ-lorraine.fr/didier.maquin`

Laboratory web site : `http://www.cran.univ-lorraine.fr`